

Original Article

Feedback control of temperature in the pyrolysis process by using microwave heating system

Yutthapong Pianroj¹, Saysunee Jumrat^{1*}, Seppo Karrila¹,
Sunisa Chuayjumnong², and Sopida Sungsoontorn³

¹ Faculty of Science and Industrial Technology, Prince of Songkla University,
Suratthani Campus, Mueang, Surat Thani, 84000 Thailand

² Major in Energy Technology, Department of Mechanical Engineering, Faculty of Engineering,
Prince of Songkla University, Hat Yai, Songkla, 91110 Thailand

³ Department of Mechanical Engineering, Faculty of Engineering,
Rajamangaha University of Technology Rattanakosin, Salaya, Phutthamonthon, Nakhon Pathom, 73170 Thailand

Received: 3 January 2020; Revised: 18 August 2020; Accepted: 26 December 2020

Abstract

Microwave (MW) heating has gained popularity because it can provide rapid and more uniform heating than conventional methods. As the pyrolysis mechanisms and products strongly depend on temperature, aside from uniformity of temperature also control of its level will strongly affect experimental results. A temperature control system was developed for use in an experimental MW cavity in which a metallic propeller driven at 50 rpm is used to scatter the MW radiation. The results show good performance of the developed feedback control system. It was experimentally tested with water at temperature set-point 80 °C; and with a pyrolysis substance (oil palm shell biomass or OPS, mixed with activated carbon or AC) at set-points 400, 500, and 600 °C. The largest bio-oil yield was obtained at the experimental conditions: ratio 70:30 at 500 °C; and the dominant chemical components found were phenol and acetic acid, as analyzed by GC-MS.

Keywords: microwave pyrolysis, microwave temperature control, oil palm shell

1. Introduction

Conventional heat is determined by the total energy in the movement of atoms or molecules of matter. Heating with MW has become a popular alternative due to its advantages in good heat transfer, the potential for high heating rates, and the ability to start or stop the heating instantaneously (Huang, Chiueh, & Lo, 2016). For heating by high-frequency waves, the sample material must absorb the energy of the waves and convert it into heat. When the molecules can be electrically polarized they will re-orient to the electromagnetic waves; these molecular vibrations absorb

energy and heat is generated by the friction between molecules throughout the material (Lam *et al.*, 2016; Salema & Ani, 2012a; Zhang *et al.*, 2017). Metals reflect MW radiation and cannot be heated with it (Huang, Chiueh, & Lo, 2016). Measurement of parameters such as temperature and moisture during MW heating is important for process control and for good quality from processing a material by heating. Therefore, studies have reported various measurement techniques to monitor the heating. Bradshaw, Delpont, and Wyk (1997) used indirect measurements, namely of electric patterns that relate to heating uniformity. Wickersheim, Sun, and Kamal (1990) designed a small standard antenna for measuring electric and magnetic fields to measure point values inside the MW cavity, and the probe was claimed to be capable of mapping field and power distribution in the processing cavity, and of monitoring on-line power changes in

*Corresponding author

Email address: saysunee.j@psu.ac.th

a process application. Belleville and Duplain (1993) adapted a novel fiberoptic thermometer using Fabry-Perot interferometry (FPI) to measure the changes of temperature, which are proportional to length changes of the fiberoptic probe from thermal expansion. A conventional thermocouple probe is generally unsatisfactory for precision temperature measurements in a MW cavity, due to electrical discharges and electromagnetic field disturbances, but there have been prior attempts to compensate for some errors in thermocouple signals from a MW environment. The benefits of using a thermocouple for temperature measurement are that this is a common and inexpensive technique, so many studies have tried to modify thermocouples for monitoring MW heating (Olmstead & Brodwin, 1997; van de Voort, Laureano, Smith, & Raghavan, 1987). Most current MW equipment operates at a frequency of 2.54 GHz. MW heating is suitable for materials that have water as a component, and moisture inside the material can be effectively heated for drying. Further, complex sample shapes do not matter, as long as the sample size is such that the waves can pass through. Typical biomass contains polar molecules that absorb MW energy (Kabir & Hameed, 2017).

At present, pyrolysis is widely used industrially, although it is not practiced in Thailand. Pianroj, Jumrat, Werapun, Karrila, and Tongurai (2016) designed bench-scale MW pyrolysis equipment to test effects on oil palm shell (OPS). However, they did not control the reactor temperature, they only controlled the MW power. Devaraju, Suresha, Ramani, and Radhakrishna (2011) developed a microcontroller-based thermogravimetric analyzer; the microcontroller controls the temperature of the furnace and communicates with the computer. Zambaldi, Magalhães, Barbosa, da Silva, and Ferreira (2017) studied the hysteresis of Thornton (IP6, IP12E, and TH5V) magnetic materials using an Arduino microcontroller to interface with the sensors. A common MW oven does not rely on temperature sensing and control. However, temperature control is essential to achieve quality targets, and feedback is necessary when the samples vary in composition and size. The availability of inexpensive microcontrollers enables implementing feedback control, making consistent (perhaps optimized) processing independent of the operator (Balogun, Oladapo, Adeoye, Kayode, & Afolabi, 2018).

An on-off temperature control system (TCS) was designed and implemented for fast pyrolysis applications of MW heating. The system was tested first with water, and then in actual high-temperature pyrolysis experiments. The design and test results are presented in this report.

2. Materials and Methods

2.1 Materials and experimental set-up

The material used to test the TCS at comparatively low temperatures was tap water, while the higher pyrolysis temperatures were tested with oil palm shell (OPS). The OPS was provided by the Green Glory Co., Ltd., Tha-Chang, Surat Thani, Thailand. Because OPS with low moisture content is a poor microwave absorber (Pianroj *et al.*, 2016), activated charcoal (AC) produced from coconut shell (which has a high dielectric loss factor, Atwater & Wheeler, 2004; Menéndez *et al.*, 2010) was used as a MW absorber. Thus, the OPS was

crushed to particle sizes from 1.18 to 2.00 mm and the AC was crushed to particle sizes around 850 μm , then dried at 105 $^{\circ}\text{C}$ to reduce the moisture content to % 8 wb. (Mushtaq, Abdullah, Mat, & Ani, 2015) and stored in zip-lock plastic bags.

2.2 Temperature control system (TCS)

The components of the temperature-controlled MW heating setup are shown in Figure 1, while the pyrolysis setup is shown in Figure 2. The experiments were carried out using a domestic multimode microwave oven, with 800 W maximum power output and 2.45 GHz frequency. A type-K thermocouple probe connected to a microcontroller board (Arduino UNO Board, MCU) was added, in order to implement feedback control of sample temperature. A magnetic relay was used to switch the MW power on or off. Further, a metallic propeller driven at 50 rpm was installed to scatter the MW radiation (Abubakar, Salema, & Ani, 2013) for improved heating uniformity. The TCS has activation limits set for controlling the temperature to within a target band. Below the lower control limit heating is turned on by releasing electrical power to the MW reactor, while when the upper limit of the band is reached the heating power is cut off. The lower control limit was to -2 $^{\circ}\text{C}$ relative to the target temperature, and the upper control limit to +2 $^{\circ}\text{C}$ relative to the target, so overall the width of the control band was 4 $^{\circ}\text{C}$. The system was typically run for a specified time.

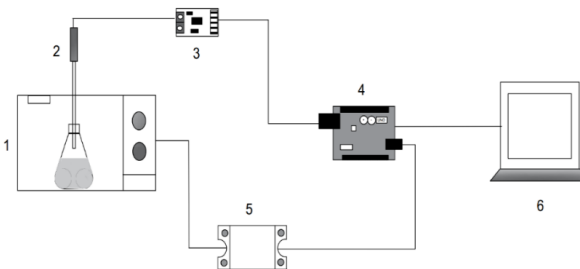


Figure 1. Components used in temperature-controlled MW heating system: (1) MW oven; (2) type-K thermocouple; (3) amplifier module MAX31855; (4) Arduino UNO; (5) solid-state relay; and (6) PC

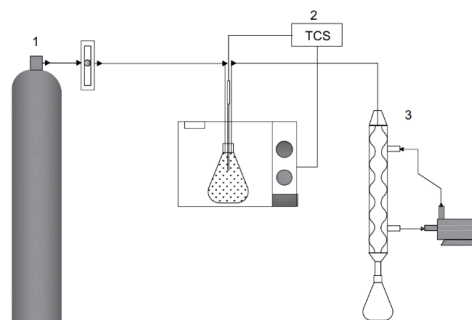


Figure 2. Setup for pyrolysis experiments: (1) nitrogen gas; and (2) TCS (3) Condensation system

2.2.1 TCS tests with water

The temperature control was tested for 80 $^{\circ}\text{C}$ set-point by heating water for 3 minutes. Ordinary tap water was

used in a 250 ml Erlenmeyer flask. The experimental run was started by connecting the computer to the MCU. Then the Arduino program was run, and a C-language command was given to load instructions into the MCU. The MCU was ready for the run when it started flashing lights on the board. Then the type-K thermocouple probe was submerged into the water to measure its temperature continuously. Data from each experimental run, with acquisition at every two seconds, was logged by a PC for later off-line analysis.

2.2.2 TCS tests with OPS and AC mix

The OPS was mixed with AC in the dry mass ratios 70:30, 80:20, and 90:10, and such samples were run with temperature set-points 400, 500, and 600 °C. Nitrogen flushing was used to remove oxygen from the reactor. The N₂ flow rate was set at four liters per minute (LPM) (Omoriyekomwan, Tahmasebi, & Yu, 2016). A condensation system collected products from the MW pyrolysis. The power output was 800 Watts and each run lasted for 30 minutes.

2.3 Quantity of products obtained from MW pyrolysis of OPS

Normally, there are three types of pyrolysis products: solid, liquid and gas (Kabir & Hameed, 2017). The yield and composition of the pyrolysis biomass depend on the properties of the raw materials, the heat to the material, the method of heating, moisture content, and other chemical components (Yin, 2012). From the experiments of OPS pyrolysis using AC as a MW absorber, the pyrolysis product yields were calculated as follows:

$$Y_{\text{bio-oil}} = \frac{M_{\text{bio-oil}}}{M_0} \times 100 \% \quad (1)$$

$$Y_{\text{char}} = \frac{M_{\text{char}}}{M_0} \times 100 \% \quad (2)$$

$$Y_{\text{gas}} = 100 \% - [Y_{\text{char}} + Y_{\text{bio-oil}}] \quad (3)$$

where, $M_{\text{bio-oil}}$ is the mass bio-oil (g), M_{char} is the mass char (g) and M_0 is the initial mass of raw material (Yin, 2012).

2.4 Analysis of liquid composition

Bio-oil samples with largest yields were subjected to GC-MS analysis using Gas Chromatograph (5977B) -Mass Spectrometer (Triple Quadrupole 7000D model), Agilent, USA, in Gas Chromatography-Electron Ionization/Mass Spectrometer (GC-EI/MS) mode to resolve the chemical compositions.

3. Results and Discussion

3.1 Temperature control with a water sample

The TCS was set at 80±2 °C for the water samples. It can be seen in Figure 3 that the temperature increased to 82 °C in about half a minute, causing the TCS to cut the MW power. When the temperature fell below 78 °C the TCS turned

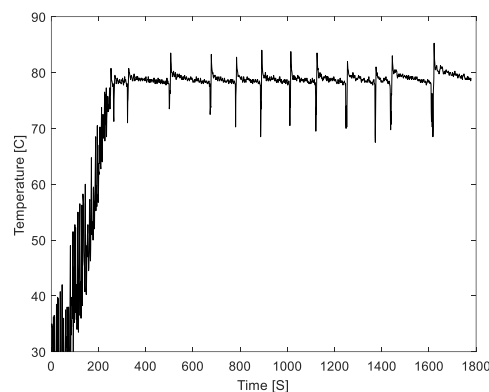


Figure 3. Time trace of temperature in a water sample with on-off regulation of MW heating

on the MW power again. This on-off feedback control of the temperature continued through the 3-minute run. The time trace also shows rapid fluctuations in temperature signal that are not physically possible, instead these indicate MW interference with the thermocouple signal. This is to be expected since an electromagnetic field will interact with a conductive material acting as an antenna. Grounding both the probe and the reactor reduced this interference, but did not completely remove it.

3.2 Temperature control of pyrolysis

Feedback control of the pyrolysis temperature was tested with OPS and AC blend samples. Feedback regulation of temperature is necessary if experimental pyrolysis runs are to be reproducible. The OPS biomass was mixed with AC in 70:30, 80:20, and 90:10 proportions. The pyrolysis temperatures tested were 400, 500, and 600 °C. AC was selected for use as a component in the mix because it absorbs MW radiation and provides fast, selective, and uniform volumetric heating (Ao *et al.*, 2018). These are benefits of mixing an MW absorber to the OPS, while differences between MW and conventional heating can be due to the different heating mechanisms between dielectric heating and conductive or convective heating. MW heating can create localized hot spots (Huang, Chiueh, Kuan, & Lo, 2016; Menéndez, Juárez-Pérez, Ruisánchez, Bermúdez, & Arenillas, 2011); moreover, flashes of light were observed on the whole sample from plasma arcs, generated by rapid localized increase in sample temperature. This phenomenon has been reported in prior literature (Omoriyekomwan *et al.*, 2016; Salema & Ani, 2012b; Wang *et al.*, 2015). The interactions of microwave irradiation with the biomass was able to locally create excited electrons and ions, and the charged ionic gas was then rapidly heated further by the MW radiation as its mass was very small relative to the energy it absorbed (Menéndez *et al.*, 2011; Wang *et al.*, 2015).

The TCS worked well, and as the temperature exceeded the upper control limit the power was cut immediately; and when the temperature became too low, the electric power was switched on quickly. Figure 4 shows the time traces of temperature using OPS and AC with temperature setpoints (A) 400 °C, (B) 500 °C, and (C) 600 °C.

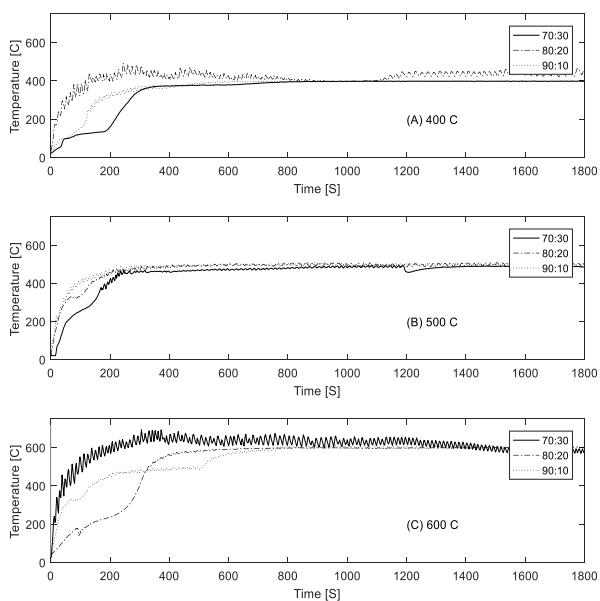


Figure 4. Time trace of temperature using OPS and AC (A) 400 °C (B) 500 °C (C) 600 °C

All three graphs show that the MW heating was very rapid (taking only a short time), which may help save time and energy. Salema and Ani (2011) reported that MW interactions depend strongly on the material properties. Bio-oil obtained from MW pyrolysis process can be adapted to serve as a renewable fuel. Patel and Kumar (2016) found that hydrothermal processing falls into two types: high-severity hydrotreating or deep hydrodeoxygenation (HDO), and low-severity hydrotreating or mild HDO. The deep HDO is related to hydroxy oxidation that begins around 350–400 °C.

The comparison of temperature characteristics between tested OPS to AC ratios showed observable effects. The properties of the material interacting with microwaves have important effects on the temperature profile (Ao *et al.*, 2018) because each material has its own characteristic MW absorbance associated with its dielectric capacity (Beneroso *et al.*, 2016; Motasemi, Afzal, & Salema, 2014; Salema *et al.*, 2013).

3.3 Product yield obtained from MW pyrolysis

Product yields of solid, liquid, and gaseous components from MW pyrolysis are shown in Table 1. In this study, the focus was on bio-oil because it is the dominant component providing potential green chemistry ingredients or bio-fuel. On the left panel of Figure 5, the average liquid yields were 33.65%, 30.70%, and 29.63% for the feedstock blend ratios 70:30, 80:20, and 90:10, respectively. The blend ratio 70:30 gave on average more liquid than the other ratios. This ratio is near optimal for OPS: AC blend. The heat transfer from AC as a MW absorber to the OPS was immediate, evidenced in Figure 4 by the steep graph slope, and a similar result can be seen in the previous work by Pianroj *et al.* (2016). In the right panel of Figure 5, the average liquid yield found was 27.92%, 34.81%, and 31.20% for 400, 500, and 600 °C temperatures, respectively. The results show that 500 °C gave higher average liquid yield than the other temperatures tested, which may be because the reactor and the condensation unit are appropriate for this temperature but had leaks at the highest temperature tested.

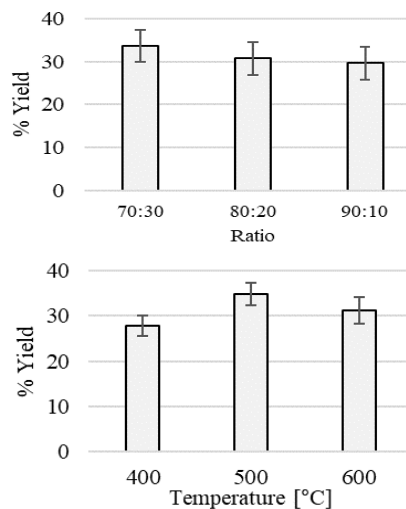


Figure 5. The average liquid yield when compared to the different ratios on the left panel and compared the different temperatures on the right panel

Table 1. Product yield obtained from the MW pyrolysis process of OPS using AC as MW absorber.

Ratio	Temperature (°C)	Product yield obtained from the MW pyrolysis process (% ± SD)		
		AC		
		Solid	Liquid (bio-oil)	Gas
70:30	400	29.05 ± 5.94	30.48 ± 4.37	40.48 ± 3.3
	500	26.67 ± 4.12	37.62 ± 3.59	35.71 ± 2.47
	600	25.24 ± 2.18	32.86 ± 2.47	41.9 ± 0.83
80:20	400	37.08 ± 9.71	26.25 ± 7.6	36.67 ± 2.6
	500	32.5 ± 2.17	32.92 ± 4.02	34.58 ± 3.15
	600	27.08 ± 0.72	32.92 ± 1.44	40 ± 1.25
90:10	400	35.56 ± 6.76	27.04 ± 2.8	37.41 ± 5.01
	500	36.67 ± 3.34	34.07 ± 3.9	29.26 ± 0.64
	600	32.59 ± 2.57	27.78 ± 1.92	39.63 ± 0.64

3.4 Chemical composition of liquid from MW pyrolysis

The liquid with largest yield (from feedstock ratio 70:30 at 500 °C) was analyzed for chemical composition by using the GC-MS. The chromatograph of mass spectrum is shown in Figure 6, and the top seven chemical components are shown in Figure 7. The dominant components in bio-oil were phenol (C₆H₆O) with 38.0% of peak area in GC-MS, and acetic acid (CH₃COOH) with 27.0% of peak area. Other smaller bio-oil components include derivatives of phenols, furan, propanone, creosol, guaiacol, and cyclopenten among others. AC promoted demethylation, decarboxylation and dehydration reactions with MW (Omoriyekomwan *et al.*, 2016). Normally, pyrolysis bio-oil from OPS is mostly composed of phenols (Asadullah, Ab Rasid, Kadir, & Azdarpour, 2013; Jeong, Lee, Chang, & Jeong, 2016; Salema & Ani, 2012a) from the decay of lignin (Mushtaq *et al.*, 2015).

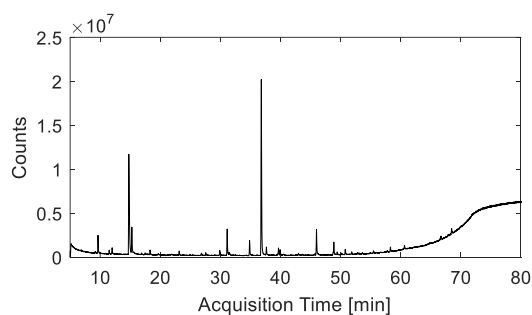


Figure 6. Chemical composition spectrum of MW pyrolyzed OPS bio-oil at a ratio of MW absorber 70:30, 500 °C, which analyzed by GC-MS

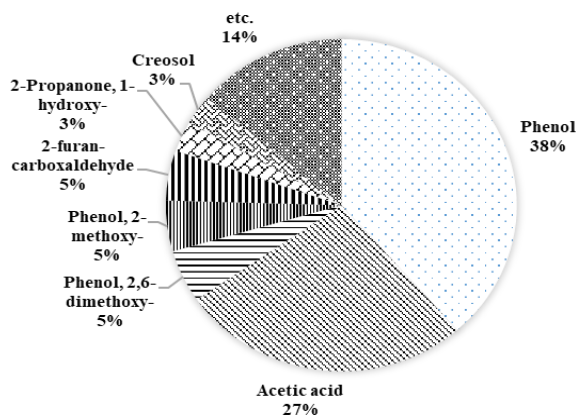


Figure 7. Chemical compositions of MW pyrolysed OPS bio-oil at a ratio of 70:30, 500 °C, which analyzed by GC-MS

4. Conclusions

A feedback control system for regulating the temperature during MW heating of laboratory-scale samples was designed and implemented. Simple on-off control was used to maintain the sample temperature within control limits. The system was tested for temperatures up to 600 °C, enabling pyrolysis with the volumetric heating by MW. The

comparison of temperature characteristics for various blend ratios of OPS to AC showed that the ratio had an effect time traces of temperature, because each material has its own MW absorbance associated with its dielectric capacity. Based on peak areas in a chromatogram, the bio-oil was 38.0% phenol and 27.0% acetic acid. The temperature control system can be developed for improved stability and more accurate temperature control, retaining on-off control implemented with a microcontroller. Eventually properly chosen operating point in MW pyrolysis may help process agricultural wastes to value-added products with economic and environmental benefits.

Acknowledgements

This work was supported by Research University Network (RUN) project from the National Research Council of Thailand (NRCT) under contact number 2559-136; subproject number 4 "Incremental bio-fuel efficient by using pyrolysis process of palm oil production waste using microwave-assisted reactor comparing to catalytic fixed bed". S.C. gratefully acknowledges the financial support from Faculty of Engineering, Prince of Songkla University, Hat-Yai, Thailand.

References

- Abubakar, Z., Salema, A. A., & Ani, F. N. (2013). A new technique to pyrolyse biomass in a microwave system: Effect of stirrer speed. *Bioresource Technology*, 128, 578-585. doi:10.1016/j.biortech.2012.10.084
- Ao, W., Fu, J., Mao, X., Kang, Q., Ran, C., Liu, Y., . . . Dai, J. (2018). Microwave assisted preparation of activated carbon from biomass: A review. *Renewable and Sustainable Energy Reviews*, 92, 958-979. doi:10.1016/j.rser.2018.04.051
- Asadullah, M., Ab Rasid, N. S., Kadir, S. A. S. A., & Azdarpour, A. (2013). Production and detailed characterization of bio-oil from fast pyrolysis of palm kernel shell. *Biomass and Bioenergy*, 59, 316-324. doi:10.1016/j.biombioe.2013.08.037
- Atwater, J. E., & Wheeler, J. R. R. (2004). Microwave permittivity and dielectric relaxation of a high surface area activated carbon. *Applied Physics A*, 79(1), 125-129. doi:10.1007/s00339-003-2329-8
- Balogun, V. A., Oladapo, B. I., Adeoye, A. O. M., Kayode, J. F., & Afolabi, S. O. (2018). Hysteresis analysis of Thornton (IP6, IP12E and TH5V) magnetic materials through the use of Arduino micro controller. *Journal of Materials Research and Technology*, 7(4), 443-449. doi:10.1016/j.jmrt.2017.05.018
- Belleville, C., & Duplain, G. (1993). White-light interferometric multimode fiber-optic strain sensor. *Optics Letters*, 18(1), 78-80. doi:10.1364/OL.18.000078
- Beneroso, D., Albero-Ortiz, A., Monzó-Cabrera, J., Díaz-Morcillo, A., Arenillas, A., & Menéndez, J. A. (2016). Dielectric characterization of biodegradable wastes during pyrolysis. *Fuel*, 172, 146-152. doi:10.1016/j.fuel.2016.01.016

- Bradshaw, S., Delpont, S., & Wyk, E. v. (1997). Qualitative Measurement of Heating Uniformity in a Multimode Microwave Cavity. *Journal of Microwave Power and Electromagnetic Energy*, 32(2), 87-95. doi:10.1080/08327823.1997.11688328
- Devaraju, J. T., Suresha, P. H., Ramani, & Radhakrishna, M. C. (2011). Development of microcontroller based thermogravimetric analyzer. *Measurement*, 44(10), 2096-2103. doi:10.1016/j.measurement.2011.08.007
- Huang, Y.-F., Chiueh, P.-T., Kuan, W.-H., & Lo, S.-L. (2016). Microwave pyrolysis of lignocellulosic biomass: Heating performance and reaction kinetics. *Energy*, 100, 137-144. doi:10.1016/j.energy.2016.01.088
- Huang, Y.-F., Chiueh, P.-T., & Lo, S.-L. (2016). A review on microwave pyrolysis of lignocellulosic biomass. *Sustainable Environment Research*, 26(3), 103-109. doi:10.1016/j.serj.2016.04.012
- Jeong, J.-Y., Lee, U.-D., Chang, W.-S., & Jeong, S.-H. (2016). Production of bio-oil rich in acetic acid and phenol from fast pyrolysis of palm residues using a fluidized bed reactor: Influence of activated carbons. *Bioresource Technology*, 219, 357-364. doi:10.1016/j.biortech.2016.07.107
- Kabir, G., & Hameed, B. H. (2017). Recent progress on catalytic pyrolysis of lignocellulosic biomass to high-grade bio-oil and bio-chemicals. *Renewable and Sustainable Energy Reviews*, 70, 945-967. doi:10.1016/j.rser.2016.12.001
- Lam, S. S., Wan Mahari, W. A., Cheng, C. K., Omar, R., Chong, C. T., & Chase, H. A. (2016). Recovery of diesel-like fuel from waste palm oil by pyrolysis using a microwave heated bed of activated carbon. *Energy*, 115, 791-799. doi:10.1016/j.energy.2016.09.076
- Menéndez, J. A., Arenillas, A., Fidalgo, B., Fernández, Y., Zubizarreta, L., Calvo, E. G., & Bermúdez, J. M. (2010). Microwave heating processes involving carbon materials. *Fuel Processing Technology*, 91(1), 1-8. doi:10.1016/j.fuproc.2009.08.021
- Menéndez, J. A., Juárez-Pérez, E. J., Ruisánchez, E., Bermúdez, J. M., & Arenillas, A. (2011). Ball lightning plasma and plasma arc formation during the microwave heating of carbons. *Carbon*, 49(1), 346-349. doi:10.1016/j.carbon.2010.09.010
- Motasemi, F., Afzal, M. T., & Salema, A. A. (2014). Microwave dielectric characterization of hay during pyrolysis. *Industrial Crops and Products*, 61, 492-498. doi:10.1016/j.indcrop.2014.07.046
- Mushtaq, F., Abdullah, T. A., Mat, R., & Ani, F. N. (2015). Optimization and characterization of bio-oil produced by microwave assisted pyrolysis of oil palm shell waste biomass with microwave absorber. *Bioresour Technol*, 190, 442-450. doi:10.1016/j.biortech.2015.02.055
- Olmstead, W. E., & Brodwin, M. E. (1997). A model for thermocouple sensitivity during microwave heating. *International Journal of Heat and Mass Transfer*, 40(7), 1559-1565. doi:10.1016/S0017-9310(96)00226-8
- Omoriyekomwan, J. E., Tahmasebi, A., & Yu, J. (2016). Production of phenol-rich bio-oil during catalytic fixed-bed and microwave pyrolysis of palm kernel shell. *Bioresource Technology*, 207, 188-196. doi:10.1016/j.biortech.2016.02.002
- Patel, M., & Kumar, A. (2016). Production of renewable diesel through the hydroprocessing of ligno cellulosic biomass-derived bio-oil: A review. *Renewable and Sustainable Energy Reviews*, 58, 1293-1307. doi:10.1016/j.rser.2015.12.146
- Pianroj, Y., Jumrat, S., Werapun, W., Karrila, S., & Tongurai, C. (2016). Scaled-up reactor for microwave induced pyrolysis of oil palm shell. *Chemical Engineering and Processing: Process Intensification*, 106, 42-49. doi:10.1016/j.cep.2016.05.003
- Salema, A. A., & Ani, F. N. (2011). Microwave induced pyrolysis of oil palm biomass. *Bioresource Technology*, 102(3), 3388-3395. doi:10.1016/j.biortech.2010.09.115
- Salema, A. A., & Ani, F. N. (2012a). Microwave-assisted pyrolysis of oil palm shell biomass using an overhead stirrer. *Journal of Analytical and Applied Pyrolysis*, 96, 162-172. doi:10.1016/j.jaap.2012.03.018
- Salema, A. A., & Ani, F. N. (2012b). Pyrolysis of oil palm empty fruit bunch biomass pellets using multimode microwave irradiation. *Bioresource Technology*, 125, 102-107. doi:10.1016/j.biortech.2012.08.002
- Salema, A. A., Yeow, Y. K., Ishaque, K., Ani, F. N., Afzal, M. T., & Hassan, A. (2013). Dielectric properties and microwave heating of oil palm biomass and biochar. *Industrial Crops and Products*, 50, 366-374. doi:10.1016/j.indcrop.2013.08.007
- van de Voort, F. R., Laureano, M., Smith, J. P., & Raghavan, G. S. V. (1987). A Practical Thermocouple for Temperature Measurement in Microwave Ovens. *Canadian Institute of Food Science and Technology Journal*, 20(4), 279-284. doi:10.1016/S0315-5463(87)71200-0
- Wang, N., Tahmasebi, A., Yu, J., Xu, J., Huang, F., & Mamaeva, A. (2015). A Comparative study of microwave-induced pyrolysis of lignocellulosic and algal biomass. *Bioresource Technology*, 190, 89-96. doi:10.1016/j.biortech.2015.04.038
- Wickersheim, K., Sun, M., & Kamal, A. (1990). A Small Microwave E-Field Probe Utilizing Fiberoptic Thermometry. *Journal of Microwave Power and Electromagnetic Energy*, 25(3), 141-148. doi:10.1080/08327823.1990.11688122
- Yin, C. (2012). Microwave-assisted pyrolysis of biomass for liquid biofuels production. *Bioresour Technol*, 120, 273-284. doi:10.1016/j.biortech.2012.06.016
- Zambaldi, E., Magalhães, R. R., Barbosa, B. H. G., da Silva, S. P., & Ferreira, D. D. (2017). Lowcost automated control for steel heat treatments. *Applied Thermal Engineering*, 114, 163-169. doi: 10.1016/j.applthermaleng.2016.11.177
- Zhang, Y., Chen, P., Liu, S., Peng, P., Min, M., Cheng, Y., . . . Ruan, R. (2017). Effects of feedstock characteristics on microwave-assisted pyrolysis - A review. *Bioresources Technology*, 230, 143-151. doi:10.1016/j.biortech.2017.01.046